Fibroblast Growth Factor Receptor 1–Transformed Mammary Epithelial Cells Are Dependent on RSK Activity for Growth and Survival

Wa Xian,[1] Leontios Pappas,[1] Darshan Pandya,[1] Laura M. Selfors,[1] Patrick W. Derksen,[4] Michiel de Bruin,[4] Nathanael S. Gray,[2] Jos Jonkers,[4] Jeffrey M. Rosen,[3] and Joan S. Brugge[1]

Departments of [1]Cell Biology and [2]Biological Chemistry and Molecular Pharmacology, Harvard Medical School, Boston, Massachusetts; [3]Department of Molecular and Cellular Biology, Baylor College of Medicine, Houston, Texas; and [4]Division of Molecular Biology, Netherlands Cancer Institute, Amsterdam, the Netherlands

Abstract

Fibroblast growth factor receptor 1 (FGFR1) is frequently amplified and highly expressed in lobular carcinomas of the breast. In this report, we evaluated the biological activity of FGFR1 in a wide range of *in vitro* assays. Conditional activation of FGFR1 in the nontransformed MCF10A human mammary cell line, MCF10A, resulted in cellular transformation marked by epidermal growth factor–independent cell growth, anchorage-independent cell proliferation and survival, loss of cell polarity, and epithelial-to-mesenchymal transition. Interestingly, small-molecule or small interfering RNA inhibition of ribosomal S6 kinase (RSK) activity induced death of the FGFR1-transformed cells, but not of the parental MCF10A cell line. The dependence of FGFR1-transformed cells on RSK activity was further confirmed in cell lines derived from mouse and human lobular carcinomas that possess high FGFR1 activity. Taken together, these results show the transforming activity of FGFR1 in mammary epithelial cells and identify RSK as a critical component of FGFR1 signaling in lobular carcinomas, thus implicating RSK as a candidate therapeutic target in FGFR1-expressing tumors. [Cancer Res 2009;69(6):2244–51]

Introduction

Invasive lobular breast carcinoma (ILC) accounts for 8% to 14% of breast cancers and is marked by linear, single-file cellular radiations and a tendency for multifocal and bilateral occurrence (1, 2). In comparison with the more common invasive ductal carcinomas (IDC), ILCs have favorable phenotypic characteristics, including higher positive status for estrogen (ER^+; 93% versus 81%, $P < 0.0001$) and progesterone receptors (PR^+; 67% versus 60%, $P < 0.0001$), diploidy (70% versus 44%, $P < 0.0001$), and low mitotic activity (69% versus 46%, $P < 0.0001$; ref. 1). However, despite this apparently favorable profile, large retrospective studies reveal that patients with ILC do not fare better than those with IDC. For example, ILC patients have a lower than expected response rate to both estrogen antagonists and chemotherapy compared with IDC patients (3, 4). In particular, whereas tamoxifen treatment is associated with a significantly increased recurrence-free survival (RFS) for ER-positive IDC ($P = 0.003$), RFS in ILC patients is not improved by tamoxifen ($P = 0.67$; ref. 5). Although the mechanisms underlying this tamoxifen resistance by ILC are unknown, these data highlight the unique properties of ILC and the need to develop alternative strategies for treatment.

Efforts to genetically define ILC have revealed amplification and high expression of fibroblast growth factor receptor 1 (FGFR1) in many of these tumors. In addition, small-molecule inhibitors of FGFR1 suppress the growth of MDA-MB-134 cells, a model of ILC, suggesting that FGFR1 signaling might represent a promising therapeutic target in a significant subset of ILC (6). Murine models of breast cancer also support a role for FGFR1 signaling in the maintenance of mammary tumors. These studies showed that altered FGFR1 activation promotes cell proliferation, increases cell survival, and alters cell polarity (7, 8). However, the significance and mechanisms of FGFR1 signaling in the pathogenesis of human breast cancer remain elusive.

To address these questions, we first generated a human mammary epithelial cell model that conditionally activates FGFR1 using a ligand-independent, dimerizer-induced activation system (7) and linked this FGFR1 activation with epidermal growth factor (EGF)–independent cell growth, suppression of anoikis, loss of cell polarity, and induction of an epithelial-to-mesenchymal transition (EMT). FGFR1 activation in MCF10A cells was shown to trigger an array of downstream signaling pathways, including p42/p44 mitogen-activated protein kinase and p90 ribosomal S6 kinases (RSK). RSK functions as a downstream effector of p42/p44 mitogen-activated protein kinase, and its activity is crucial for FGFR3-mediated hematopoietic transformation (9). Moreover, RSK has been implicated in antiapoptotic signaling (10) and in stimulating breast carcinoma proliferation (11). We therefore asked whether RSK function is critical for FGFR1-mediated mammary epithelial cell transformation in our model. Indeed, inhibition of RSK activity effectively abolished the proliferation and ultimately the survival of FGFR1-transformed MCF10A cells but had no obvious effect on the growth or viability of the parental cell line. Moreover, the selective sensitivity to RSK inhibition was also observed in mouse and human lobular carcinoma cell lines with high FGFR1 activity. Thus, lobular carcinomas with aberrant FGFR1 activity display characteristics of "addiction" to RSK signaling that normal cells lack (12–14), and therefore, RSK may represent a novel drug target for the patients with ILC.

Materials and Methods

Cell lines and cell culture. MCF-10A cells were obtained from the American Type Culture Collection and cultured as described[5] (15) in growth

Note: Supplementary data for this article are available at Cancer Research Online (http://cancerres.aacrjournals.org/).

Current address for P.W. Derksen: Department of Medical Oncology, University Medical Center, Utrecht, the Netherlands.

Requests for reprints: Joan S. Brugge, Department of Cell Biology, Harvard Medical School, 240 Longwood Avenue, Boston, MA 02115. Phone: 617-432-3974; Fax: 617-432-3969; E-mail: joan_brugge@hms.harvard.edu.

doi:10.1158/0008-5472.CAN-08-3398

[5] http://brugge.med.harvard.edu/

medium containing DMEM/F12 (Invitrogen) supplemented with 5% donor horse serum, 20 ng/mL EGF, 10 μg/mL insulin, 100 μg/mL hydrocortisone, 1 ng/mL cholera toxin, 50 units/mL penicillin, and 50 mg/mL streptomycin. Hemagglutinin-tagged bovine iFGFR1 cDNA was subcloned into the pBABE-Puro retroviral vector as described before (8). MCF-10A cells expressing the iFGFR1 were generated by retroviral gene transfer. Stable populations were obtained by selection with 2 μg/mL puromycin (Sigma-Aldrich).

Immunoblots. Cell lysates were prepared in NP40 lysis buffer [50 mmol/L Tris (pH 7.6), 150 mmol/L NaCl, 1% NP40, 10% glycerol] supplemented with leupeptin (2 μg/mL), aprotinin (2 μg/mL), phenylmethylsulfonyl fluoride (1 mmol/L), NaF (50 mmol/L), and Na_3VO_4 (1 mmol/L). Lysates were cleared by centrifugation at 16,000 × *g* for 15 min at 4°C, and the supernatant was used for all subsequent procedures. Lysates were separated by SDS-PAGE and transferred to either nitrocellulose or polyvinylidene difluoride membranes. Immunoblotting was done according to the antibody manufacturers' recommendations using enhanced chemiluminescence. Antibodies used for immunoblotting were anti–phospho-Akt (S473), anti–phospho-p70S6K (T389), anti–phospho-extracellular signal-regulated kinase (ERK), and anti–phospho-RSK (Thr^{359}/Ser^{363}; Cell Signaling) and antitubulin (Sigma-Aldrich). Cells were cultured in DMEM/F12 medium for 24 h before being stimulated with dimerizer at the indicated time points. Immunoprecipitation was carried out using the Catch and Release reversible immunoprecipitation system following the manufacturer's protocol (Upstate).

Invasion assay. Growth medium (0.5 mL) was added to the wells of a 12-well plate (Falcon). Ten thousand iFGFR1-expressing MCF10A cells were plated in 0.5 mL of growth medium in 12-well format cell culture 8-μm pore inserts coated with Matrigel (Falcon). After a 20-h incubation, cells that had not migrated through the filters were removed using a cotton swab and the filters were stained with 4′,6-diamidino-2-phenylindole (DAPI) and the nuclei were counted.

Growth curves. MCF-10A cells expressing iFGFR1 were seeded in triplicate at 25×10^3 per well in 12-well plates on day 0 in growth medium in the presence or absence of EGF, dimerizer, or 1-(4-amino-7-(3-hydroxypropyl)-5-*p*-tolyl-7*H*-pyrrolo[2,3-*d*]pyrimidin-6-yl)-2-chloroethanone (CMK). Cells were trypsinized and counted with a hemacytometer on days 1, 4, 7, and 10. Fresh medium was changed on the same days.

Colony formation in soft agar assay. To assess anchorage-independent growth, triplicate samples of 5×10^4 cells from MCF10A cells expressing iFGFR1 or MDA-MB-134 cells were mixed 4:1 (v/v) with 2.0% agarose in MCF-10A growth medium for a final concentration of 0.4% agarose. The cell mixture was plated on top of a solidified layer of 0.5% agarose in growth medium. Cells were fed every 6 to 7 d with growth medium containing 0.4% agarose in the presence or absence of dimerizer and 1 μmol/L CMK. Cells were stained with 0.02% iodonitrotetrazolium chloride (Sigma-Aldrich). Colonies in the entire well larger than 50 μm were counted using a dissecting microscope.

Anoikis assay. Detachment-induced cell death was assayed essentially as described (16). Six-well tissue culture plates were coated with 6 mg/mL poly-HEMA in 95% ethanol, incubated at 37°C for several days until dry, and rinsed with PBS. MCF-10A cells expressing iFGFR1 or mouse lobular carcinoma cell lines were then plated at 400,000 per well in 2 mL growth medium with or without dimerizer or CMK for 42 h. Cells were collected and washed with PBS. Apoptosis was measured using a Cell Death Detection ELISA kit according to the manufacturer's instructions (Roche Diagnostics). Cells were lysed in 200 μL lysis buffer supplied with the kit and 20 μL lysate was used in the assay. Absorbance at 405 nm was measured and reported as arbitrary units.

Morphogenesis assay. The three-dimensional culture of MCF-10A cells or a variety of different breast cancer cell lines on basement membrane was carried out as described previously (15, 17). Briefly, 5×10^3 cells were resuspended in growth medium containing 2% Matrigel (BD Biosciences) with or without dimerizer or CMK and seeded on top of a layer of growth factor–reduced Matrigel. Medium was exchanged every 4 d. CMK (1 μmol/L) was added to cultures as indicated on day 0 or day 6 of three-dimensional culture and exchanged every 4 d thereafter. Photographs of representative fields were taken on day 10. Ethidium bromide staining was carried out as described previously (15).

Indirect immunofluorescence and image acquisition. The following primary antibodies were used for indirect immunofluorescent detection of specific antigens: anti-cleaved caspase-3 (Asp^{175}; Cell Signaling Technology), anti-CD49f (Cell Signaling Technology), anti–E-cadherin (Transduction Laboratories), and anti-FGFR1 (Santa Cruz Biotechnology); all first antibodies were used at a dilution of 1:200. Secondary antibodies were as follows: anti-mouse or anti-rabbit coupled with Alexa Fluor dyes (Invitrogen). All secondary antibodies were used at a dilution of 1:500. Nuclei were stained with DAPI (Invitrogen). Immunostaining was performed as previously described (15). Tissue microarray was deparaffinized and immunostaining was done with sodium citrate antigen retrieval. Confocal analyses were performed using a Nikon C1 laser-scanning confocal microscope. The acquisition software used was MetaMorph image analysis software. Phase-contrast images were captured using an inverted microscope (Nikon TE300). The acquisition software used was ImageJ.

Small interfering RNA. SMARTpool small interfering RNA (siRNA) for RSK1 or RSK2 and siGLO RISC-free siRNA as the control were introduced into subconfluent (75–80%) iFGFR1-expressing MCF10A cells or mouse lobular carcinoma cell lines using DharmaFECT transfection reagent (Dharmacon) according to the manufacturer's instructions. After 24 h, the media were changed to regular growth media.

Results

FGFR1 is highly expressed in a subset of invasive lobular carcinomas. In a previous study, FGFR1 was shown to be concurrently amplified and overexpressed in 7 of 13 cases of lobular carcinoma examined (6). Mining of a data set from the Gene Expression Omnibus[6] that contained 32 IDC and 20 ILC tumors (18) revealed that FGFR1 RNA expression was significantly (P = 0.029) more highly expressed in ILC compared with IDC (Fig. 1*A*). To examine protein expression of FGFR1 in ILC in a larger cohort of tumors, we performed immunofluorescence analysis of FGFR1 expression in two independent sets of human ILC using tissue microarrays that were purchased from U.S. Biomax, Inc. (BR805 and BR809).[7] The FGFR1 antibody specificity was verified in breast cancer cell lines (Supplementary Fig. S1*A*). Among 147 tumor samples, 42 (28%) displayed strong staining for FGFR1 in tumor cells, with no detectable staining in tumor stroma (Fig. 1*B*; Supplementary Fig. S1*B*). These results provide strong support for earlier studies that showed an association of FGFR1 with lobular carcinomas (6).

iFGFR1 activation transforms MCF10A cells. To determine whether FGFR1 activation can transform human mammary epithelial cells, we generated stable pools of MCF10A mammary epithelial cells expressing iFGFR1 by retroviral infection. The iFGFR1 transgene contains a FGFR1 kinase domain fused with F36V mutant FKBP12 (FKBPv). The bivalent compound AP20187 (dimerizer) exhibits high affinity for the FKBPv domain and induces FGF ligand-independent dimerization of the FGFR1 kinase domains. Phosphorylation of iFGFR1 following dimerization was detected by Western blot and immunofluorescence staining using specific antibodies targeting phosphorylated FGFR1 at $Tyr^{653/654}$ or Tyr^{766} (Supplementary Fig. S2*A* and *B*). Consequently, iFGFR1 dimerization led to activation of downstream signaling pathways reflected in the induction of phosphorylation of p70S6K, Akt, p42/p44 mitogen-activated protein kinase, and p90 RSKs (Fig. 2*A*).

The proliferation of MCF10A cells requires EGF in the growth medium and this requirement can be overcome by ectopic

[6] http://www.ncbi.nlm.nih.gov/geo/query/acc.cgi?acc=GSE3971
[7] http://www.biomax.us/tissue-arrays/Breast

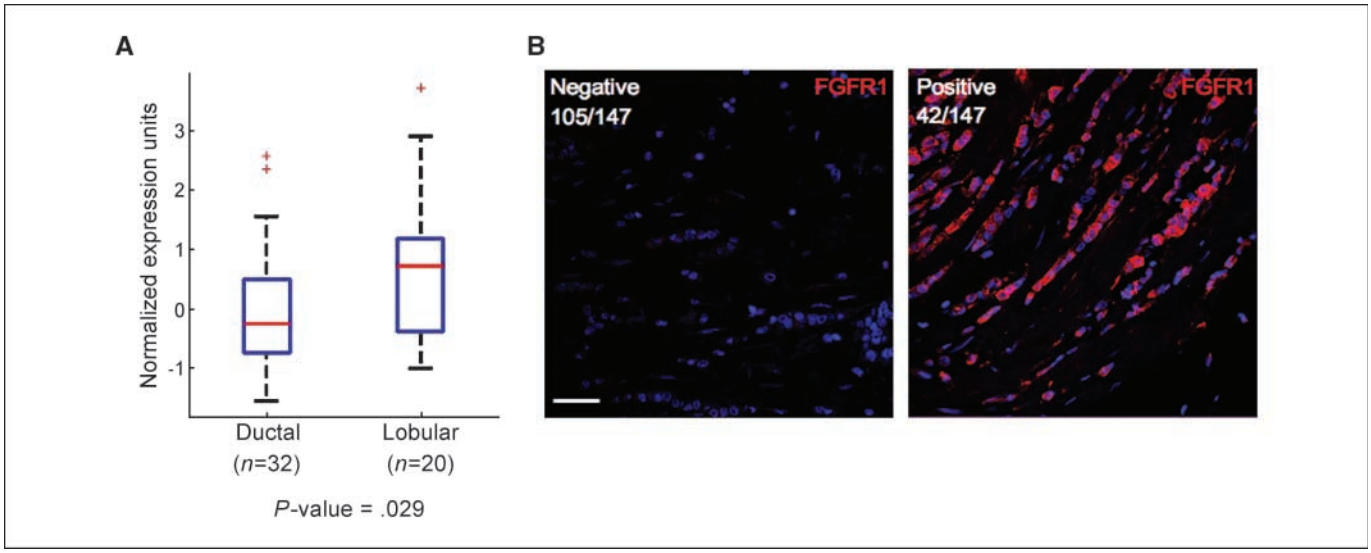

Figure 1. FGFR1 expression in lobular carcinoma. *A,* analysis of FGFR1 expression in ductal and lobular carcinomas via gene expression microarray. Box plots and two-sample *t* statistics of the normalized log ratios of gene expression levels for ILCs and IDCs were generated using JMP 7.0. *B,* representative confocal images from lobular carcinoma tissue microarrays BR805 and BR809 stained with an antibody to FGFR1 (*red*). Nuclei were stained with DAPI (*blue*). *Bar,* 50 μm.

expression of certain oncogenes (15). We, therefore, tested whether activation of iFGFR1 in MCF-10A cells was sufficient to allow for EGF-independent growth. In cells treated with dimerizer to activate iFGFR1, there was no difference in proliferation relative to the untreated iFGFR1-expressing cells when EGF was maintained in the growth medium. However, only the dimerizer-treated, but not untreated, iFGFR1-expressing MCF10A cells were able to proliferate in the absence of EGF (Fig. 2*B*).

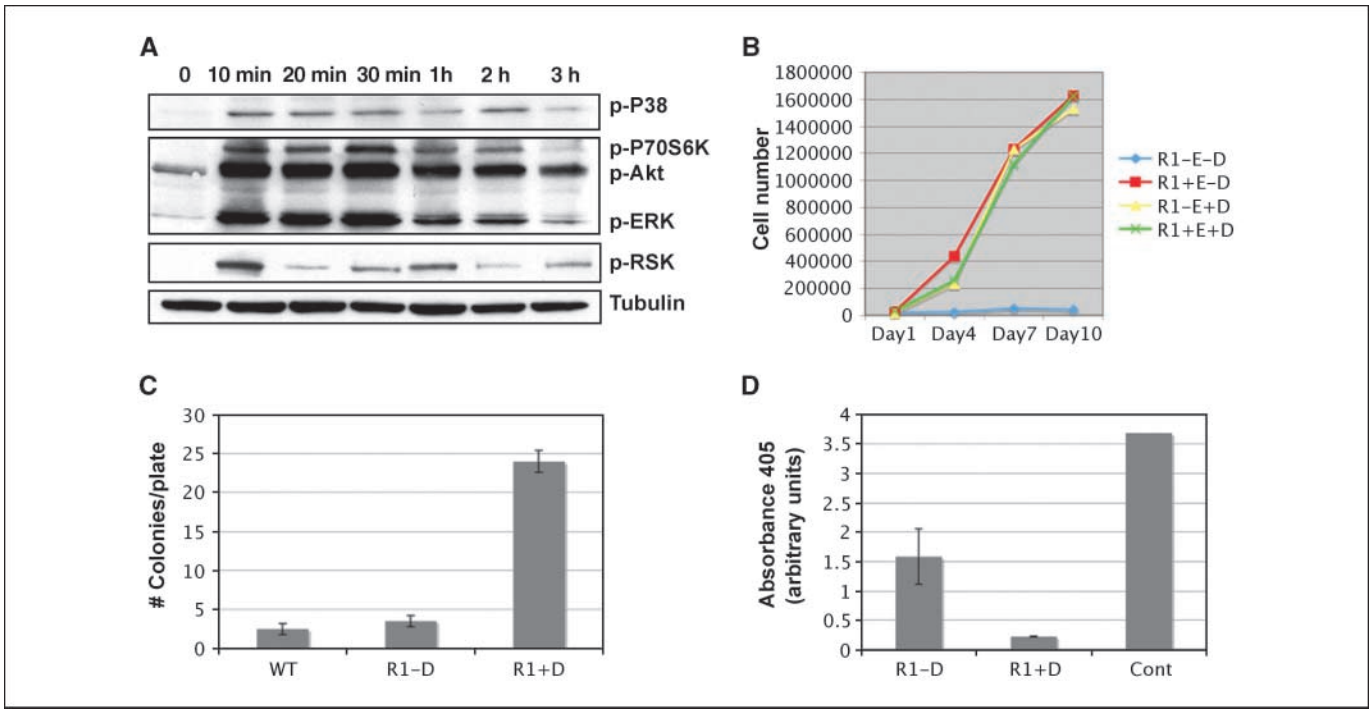

Figure 2. iFGFR1 activation in MCF10A cells induces multiple phenotypes characteristic of breast tumor cells. *A,* time course of signaling following iFGFR1 activation. MCF10A cells expressing iFGFR1 were incubated in starvation medium lacking EGF and insulin for 24 h and then stimulated for the indicated times. Lysates were immunoblotted with phospho-specific antibodies as indicated. Tubulin was probed as a loading control. *B,* EGF-independent cell growth. MCF-10A cells expressing iFGFR1 were incubated in growth medium ± EGF and ± dimerizer (*D*) on day 0 and cell numbers were plotted for each day indicated. *C,* histogram of soft agar colony formation. WT MCF10A cells or MCF10A cells expressing iFGFR1 were mixed with agarose in growth medium and plated in six-well plates with and without the iFGFR1 dimerizer. Colonies in the entire well were counted using a dissecting microscope. *Columns,* mean of triplicate wells for each sample from a representative experiment; *bars,* SD. *D,* escape from anoikis. Cells were cultured in suspension in poly-HEMA–coated plates for 42 h and apoptosis was measured using the Cell Death ELISA kit. Results are plotted on histogram as arbitrary units of absorbance at 405 nm. Greater absorbance indicates greater apoptosis and histone release. *Columns,* mean of triplicate wells for each sample from a representative experiment; *bars,* SD.

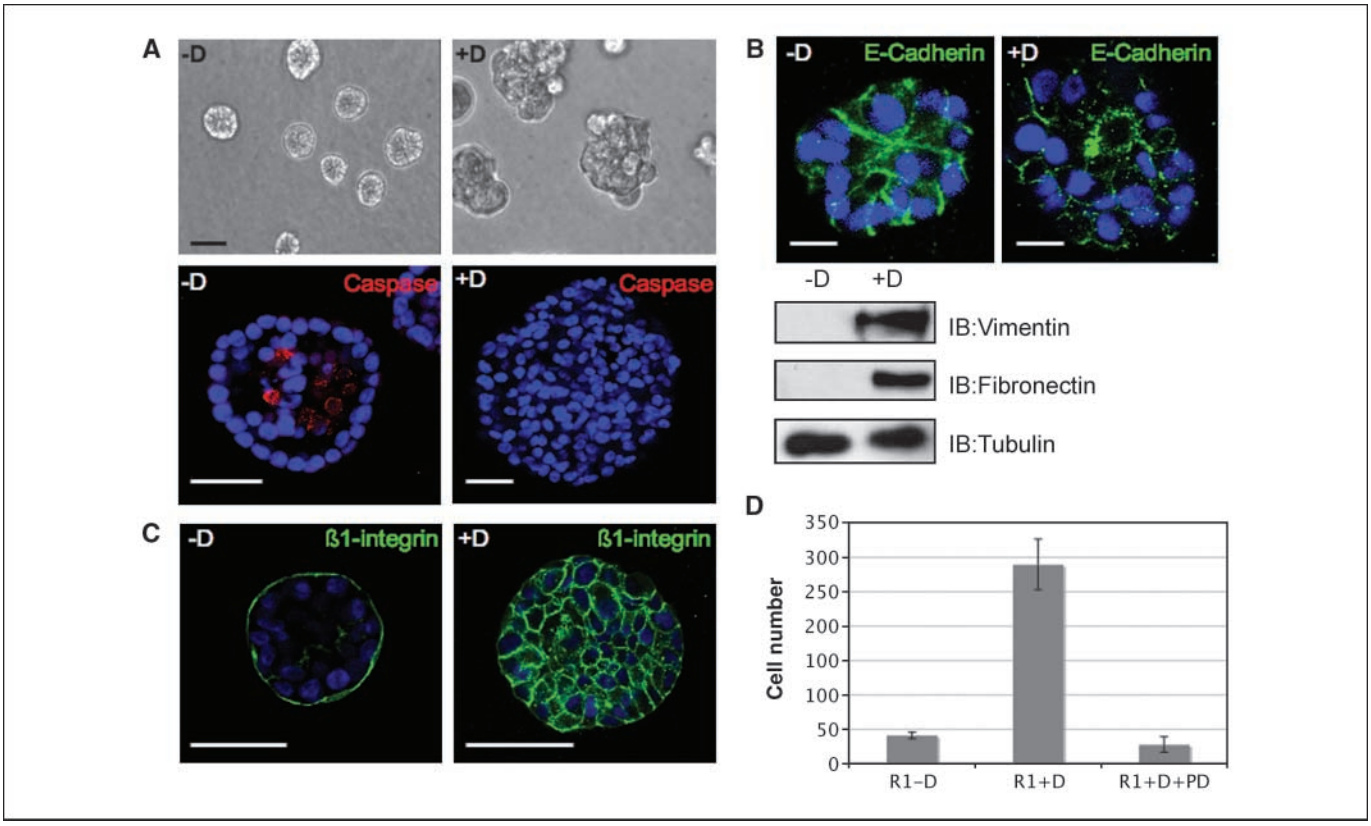

Figure 3. iFGFR1 activation induces altered three-dimensional morphogenesis, EMT, and cell polarity disruption. *A,* MCF-10A cells expressing iFGFR1 were cultured in Matrigel as described in Materials and Methods. *Top,* 10-d-old iFGFR1 structures were grown in the absence (−D) or presence of dimerizer (+D). Bright-field images of structures are shown. *Bar,* 100 μm. *Bottom,* representative confocal images of day 10 iFGFR1 structures −D/+D stained with antibodies detecting cleaved caspase-3 (*red*). DAPI (*blue*) marked the nuclei. *Bar,* 50 μm. *B, top,* representative confocal images of the day 10 iFGFR1 structures −D/+D stained with antibodies detecting E-cadherin (*green*), and DAPI (*blue*) was used to mark nuclei. *Bar,* 20 μm. *Bottom,* immunoblotting was performed on protein extracts from three-dimensional cultures of MCF10A cells expressing iFGFR1 −D/+D. *C,* representative confocal images of the day 10 iFGFR1 structures −D/+D stained with antibodies detecting β1-integrin (*green*), and DAPI (*blue*) was used to label nuclei. *Bar,* 50 μm. *D,* cell invasion. Cells expressing iFGFR1 were seeded in Transwell invasion chamber −D/+D and incubated for 18 h, and the invading cells were counted. For assays with the FGFR inhibitor PD173074, cells were incubated with inhibitor for 15 min before plating. Experiments were repeated a minimum of three times.

Anchorage-independent survival and proliferation is another common feature of cellular transformation. The dimerizer-treated, but not untreated, iFGFR1-expressing MCF10A cells were able to form colonies in soft agar, showing that FGFR1 activation induces anchorage-independent growth in mammary epithelial cells (Fig. 2*C*). Moreover, in contrast to the untreated iFGFR1-expressing MCF10A cells, the treated iFGFR1-expressing cells displayed anchorage-independent survival by escaping anoikis, a process through which epithelial cells undergo apoptosis when detached from the extracellular matrix. iFGFR1 activation in MCF10A cells resulted in an 80% reduction in anoikis compared with control cells (Fig. 2*D*).

iFGFR1 activation disrupts MCF10A morphology in three-dimensional culture. To further investigate the effects of iFGFR1 activation on transformation of mammary epithelial cells, we examined the morphology of iFGFR1-activated cells in three-dimensional culture. When cultured in reconstituted basement membrane (Matrigel), MCF10A mammary epithelial cells form spherical structures that consist of an outer layer of polarized, growth-arrested epithelial cells surrounding a hollow lumen, which mimics the normal cellular architecture present in the mammary gland. In contrast, iFGFR1-activated MCF10A cells formed large and disorganized structures in Matrigel, similar to that previously observed in the iFGFR1-activated mouse mammary HC11 cell line (8). In addition, treatment with the selective FGFR inhibitor PD173074 prevented the iFGFR1-induced disruption of morphogenesis (Fig. 3*A*; Supplementary Fig. S3*A*). To examine whether iFGFR1 activation can promote luminal cell survival, apoptosis was analyzed by immunostaining with an antibody to activated caspase-3. In comparison with the untreated iFGFR1 structures, a dramatic decrease in the number of cells staining positive for activated caspase-3 was detected in the luminal cells of the structures treated with the dimerizer (Fig. 3*A*). Similar results were obtained by vital staining with ethidium bromide, which stains dying cells; iFGFR1 activation reduced luminal apoptosis to 20% that of controls (Supplementary Fig. S3*B*).

iFGFR1 activation causes EMT and loss of cell polarity. In three-dimensional culture, MCF10A cells displayed high levels of membrane-localized E-cadherin and little or no expression of the mesenchymal markers vimentin or fibronectin. However, iFGFR1-activated MCF10A cells in three-dimensional culture displayed lower levels of E-cadherin, and E-cadherin was mislocalized to the cytoplasm as punctate staining (Fig. 3*B*). In addition, the expression of vimentin and fibronectin was highly induced following iFGFR1 activation in these cells (Fig. 3*B*). As EMT is usually accompanied by a loss of cell polarity, we monitored this property using an antibody to β1-integrin, which in the untreated iFGFR1-expressing cells is restricted to the basolateral surfaces.

Significantly, iFGFR1 activation was accompanied by a loss of β1-integrin polarity (Fig. 3*C*), a feature consistent with cells undergoing EMT. One phenotypic consequence of EMT is enhanced cell migration and invasion. In Transwell chamber assays, the iFGFR1-activated MCF10A cells were indeed able to migrate and invade ~6-fold more than the iFGFR1-expressing cells without the dimerizer treatment (Fig. 3*D*).

RSK inhibition suppresses FGFR1-dependent cell growth and survival. RSK has been implicated in FGFR3-mediated hematopoietic transformation (9). To examine whether RSK is also a critical downstream signaling effector of FGFR1-mediated mammary epithelial transformation, we used a reported irreversible RSK inhibitor, CMK, designed to selectively target the paired threonine/reactive cysteine uniquely found in the COOH-terminal domain of RSK (19). Although the pyrrolopyrimidine scaffold used to generate CMK inhibited Src family kinases, CMK itself is highly selective for RSK (IC_{50}, 15 nmol/L compared with 4 μmol/L for the Src family kinase Fyn; ref. 18). We found that inhibition of RSK by CMK inhibited the proliferation of iFGFR1-transformed MCF10A cells, but not that of nontransformed iFGFR1-expressing cells, in the absence of dimerizer in both two-dimensional and three-dimensional cultures (Fig. 4*A* and *B*). Moreover, we observed that inhibition of RSK kinase activity by CMK at a concentration of 1 μmol/L abolished the escape from anoikis conferred by iFGFR1 (Fig. 4*C*). To confirm the requirement for RSK by an independent method, we used pools of siRNA targeting RSK1 and RSK2 mRNAs to specifically knock down their expression in MCF10A cells (Fig. 4*D*). Cotransfection of RSK1 and RSK2 siRNA pools significantly decreased iFGFR1-mediated, anchorage-independent cell survival (Fig. 4*D*). To distinguish between the involvement of RSK1 versus RSK2 in a transforming activity of FGFR1, their expression was specifically knocked down individually (Supplementary Fig. S4*A*). Loss of RSK1, but not RSK2, expression abolished FGFR1-mediated cell survival of matrix-deprived cells, suggesting a more dominant role of RSK1 in FGFR1 signaling pathway (Supplementary Fig. S4*B*). Kang and colleagues (9) showed that FGFR3 directly phosphorylates RSK2 and that this phosphorylation is required for ERK-mediated phosphorylation and activation. Although our data support the concept that RSK1 is functionally downstream of FGFR1, further biochemical studies are necessary to determine whether RSK1 is a direct target of FGFR1. However, inhibition of mitogen-activated protein/ERK kinase (MEK)/ERK signaling by U0126 abolished iFGFR1-mediated, anchorage-independent cell survival and cell transformation in three-dimensional cultures,

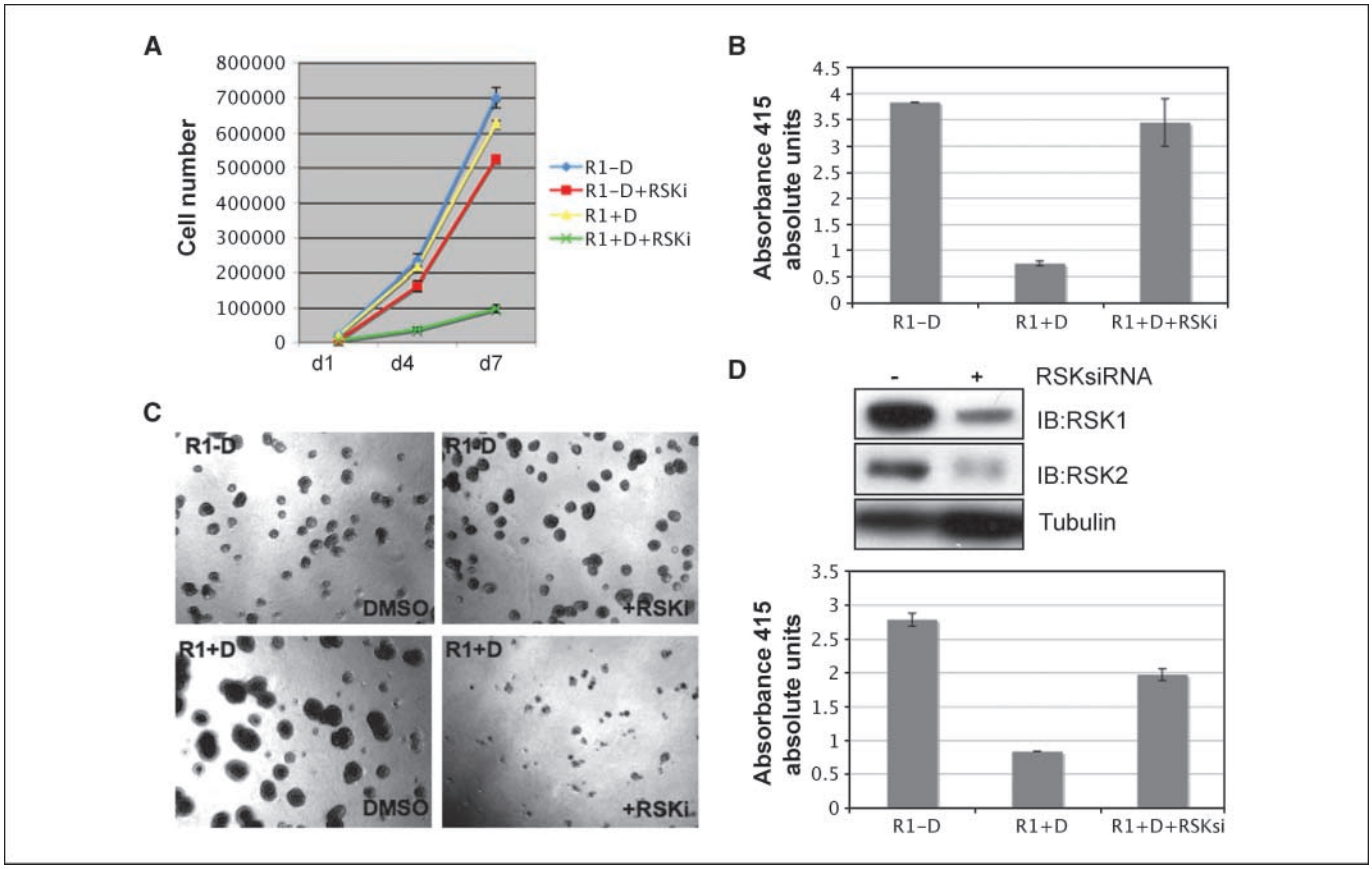

Figure 4. RSK activity is critical for iFGFR1-dependent cell growth and survival. *A,* growth curve of MCF-10A cells expressing iFGFR1 in growth medium with or without dimerizer and CMK, a selective RSK inhibitor. *B,* histogram of anoikis in cells cultured in medium with or without dimerizer and CMK. Apoptosis was measured using the Cell Death ELISA kit. Results are plotted as arbitrary units of absorbance at 405 nm. Greater absorbance indicates greater apoptosis and histone release. *Columns,* mean of triplicate wells for each sample from a representative experiment; *bars,* SD. *C,* phase-contrast images of MCF10A cells expressing iFGFR1 cultured on Matrigel with and without dimerizer and RSK inhibitor. Representative bright-field images of structures were taken on day 10. *D, top,* Western blot of RSK1 and RSK2 expression in iFGFR1 MCF10A cells following RSK1- and RSK2-specific siRNA transfection; *bottom,* anoikis in cells with and without RSK siRNA. Apoptosis was measured using the Cell Death ELISA kit. Results are plotted as arbitrary units of absorbance at 405 nm. *Columns,* mean of triplicate wells for each sample from a representative experiment; *bars,* SD.

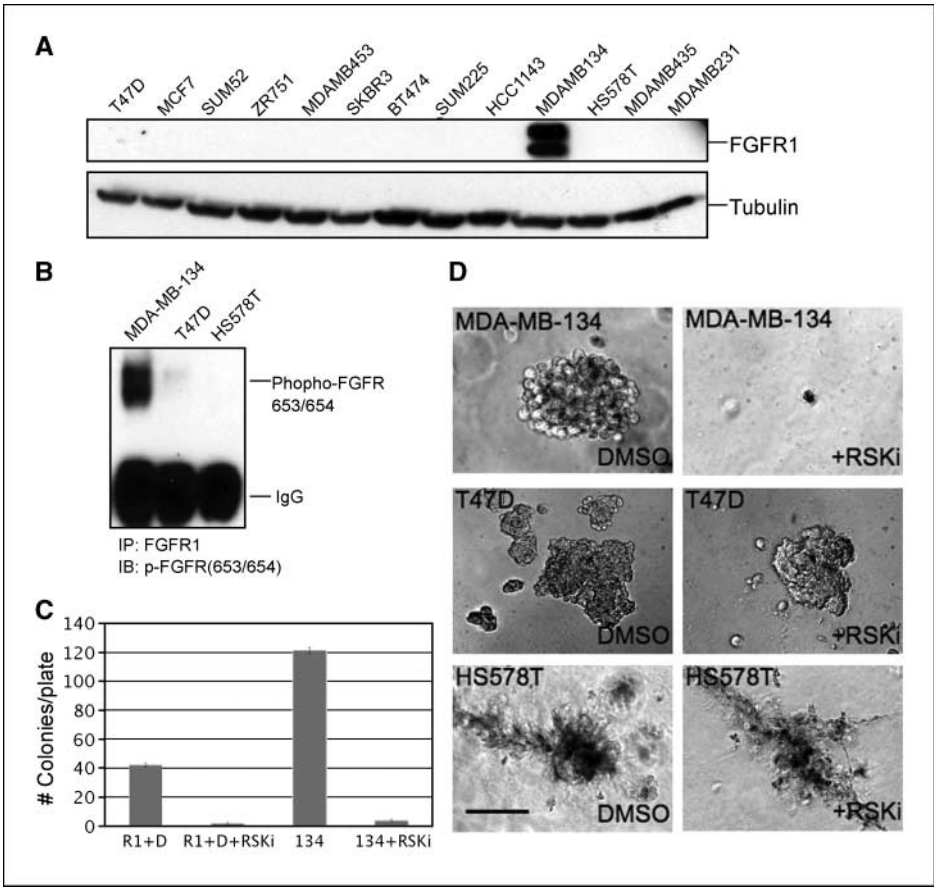

Figure 5. RSK activity is essential for the growth and survival of MDA-MB-134 cells. *A,* Western blot of extracts of 13 breast cancer cell lines was probed with an antibody to FGFR1. Antitubulin was used as loading control. *B,* Western blot of immunoprecipitated FGFR1 from three breast cancer cell lines revealed by an antibody phospho-FGFR $Tyr^{653/654}$. *C,* soft agar colony formation of MCF-10A cells expressing activated iFGFR1 or MDA-MB-134 cells with and without the RSK inhibitor CMK. Colonies in the entire well were counted using a dissecting microscope. *Columns,* mean of triplicate wells for each sample from a representative experiment; *bars,* SD. *D,* phase-contrast images of MDA-MB-134, T47D, and HS578T cells grown on Matrigel with or without the RSK inhibitor CMK. *Bar,* 100 μm.

recapitulating the effects of RSK inhibition (Supplementary Fig. S5*A* and *B*). These data, together with the fact that RSK is a downstream effector of MEK/ERK signaling cascade (20), support the importance of the ERK-RSK pathway in iFGFR1-mediated mammary epithelial cell transformation.

MDA-MB-134 cell growth depends on RSK activity. To identify additional cellular models of FGFR1 activation, we screened 13 breast cancer cell lines with anti-FGFR1 antibodies. Only one of these cell lines, MDA-MB-134, showed strong FGFR1 expression and phosphorylation (Fig. 5*A* and *B*). MDA-MB-134 cells have been previously used as a model for the study of ILC cells that express high levels of FGFR1 amplification and overexpression (6, 21). To examine whether RSK activity is important for anchorage-independent cell growth of MDA-MB-134 cells, these cells and MCF10A cells with activated iFGFR1 were grown in soft agar with and without 1 μmol/L CMK. Significantly, CMK abolished colony formation of both cell populations (Fig. 5*C*). Moreover, RSK activity proved critical for the growth of MDA-MB-134 cells in Matrigel, whereas the growth of T47D and HS578T cells that did not express FGFR1 was insensitive to CMK (Fig. 5*D*).

RSK activity is essential for the growth and survival of a murine lobular carcinoma cell line. Tissue-specific deletion of *E-cadherin* and *p53* genes in mice resulted in metastatic mammary carcinomas that strongly resemble human ILC (22). We probed seven cell lines derived from the WAPcre;Cdh1;Trp53 mice[8] to determine whether they expressed FGFR1 activity. Among these cell lines, the WEP7 cell line displayed high FGFR1 tyrosine phosphorylation (Fig. 6*A*). Notably, immunofluorescence staining showed that FGFR1 expression was up-regulated in the primary tumor from which the WEP7 cell line was derived, but not in the other tumors (Fig. 6*B*).

To test whether RSK kinase activity is required for the growth of WEP7 cells in three-dimensional cultures, we compared their ability to grow in Matrigel in the presence and absence of CMK with that of WEP4 cells, which do not express high FGFR1. CMK suppressed the growth of WEP7 cells, but not that of WEP4 cells (Fig. 6*C*). Consistent with this observation, RSK1 and RSK2 siRNAs inhibited the growth of WEP7 cells but had little effect on WEP4 cells (Fig. 6*C*). We further examined three-dimensional colonies of WEP7 cells in Matrigel and found that the addition of CMK to 6-day-old WEP7 structures induced the activation of caspase-3 and the formation of a lumen in these normally solid spheres (Fig. 6*D*).

Moreover, we observed that inhibition of RSK kinase activity in WEP7 cells by CMK at a concentration of 1 μmol/L resulted in a 2.5-fold induction of anoikis compared with untreated WEP7 cells (Fig. 6*D*), suggesting that RSK kinase activity is required for the anchorage-independent cell survival of WEP7 cells.

Discussion

In this study, we investigated multiple breast cancer models distinguished by abundant FGFR1 expression and found that in each case FGFR1 overexpression correlated with a dependency on RSK activity for multiple transformation variables. Therefore, pharmacologic inhibition of RSK might represent a strategy for

[8] P.W. Derksen et al., in preparation.

treating lobular breast carcinomas and other cancers marked by excessive FGFR1 expression.

Altered expression of receptor tyrosine kinases (RTK), such as EGF receptor (EGFR), ErbB2, vascular endothelial growth factor receptor, and Ret, has been implicated in the development of cancer, and as a group, these receptors represent important targets for monoclonal antibodies and small-molecule inhibitors for treatment of a wide range of cancers (23, 24). Indeed, in breast cancer, antibodies to the EGFR isoform Her2 have been shown to dramatically reduce the recurrence of Her2-expressing cancers (25). Recently, systematic sequencing of cancer genomes has revealed that the FGF signaling pathway displays the highest enrichment for kinases carrying nonsynonymous mutations among 537 nonredundant pathways that were examined (26). Moreover, studies in a variety of cancers, such as breast, bladder, pancreatic, and prostate cancers, suggest that FGF signaling is a promising target in multiple malignancies (16, 27–29). This is consistent with the emerging evidence suggesting that specific genotypes, as opposed to tissue types, should be considered as part of the development and clinical evaluation of molecularly targeted cancer drugs (30). Our study not only validates the previous studies of FGFR1 expression in mouse breast cancer models that showed that FGFR1 activation leads to hyperplasia and invasive lesions *in vivo* and tumor cell characteristics *in vitro* (7, 8) but also points to a downstream signaling effector of FGFR1, RSK, as alternative therapeutic target.

Evidence supporting the critical coupling of FGFR1 and RSK in oncogenic transformation was derived from three independent models. In the first model, involving the conditional induction of FGFR1 activity in the immortalized, nontransformed breast epithelial cell line MCF10A, FGFR1 transformation rendered the cells vulnerable to a RSK inhibitor that had no effect on the parental MCF10A cells. In a second model, we found that the human breast cancer line MDA-MB-134, which highly expresses FGFR, is also sensitive to the RSK inhibitor. Finally, a FGFR1-expressing cell line derived from a $p53^{-/-}$; $Cdh1^{-/-}$ mouse lobular carcinoma also exhibited dependence on RSK activity. Thus, the dissection of the downstream signaling pathways of FGFR1 that are critical for induction of transformed phenotypes using the MCF10A system, together with several mouse and human tumor models having high FGFR1 expression, suggest an acquired dependence on RSK by such cells.

With regard to targeting RSK activity, several small molecules have been developed. For example, the natural product SL0101 from the tropical plant *Forsteronia refracta* (11) and BI-D1870 (31) specifically target the NH_2-terminal kinase domain of RSK. The irreversible CMK and FMK inhibitors were designed to specifically target the COOH-terminal, autophosphorylation kinase domain of RSK by alkylating Cys^{436} located in the ATP-binding site (19, 32). The CMK insensitivity of wild-type (WT) MCF10A cells and a variety of human and mouse breast cancer cells lacking FGFR1 expression suggests that FGFR1-mediated breast cancer cell

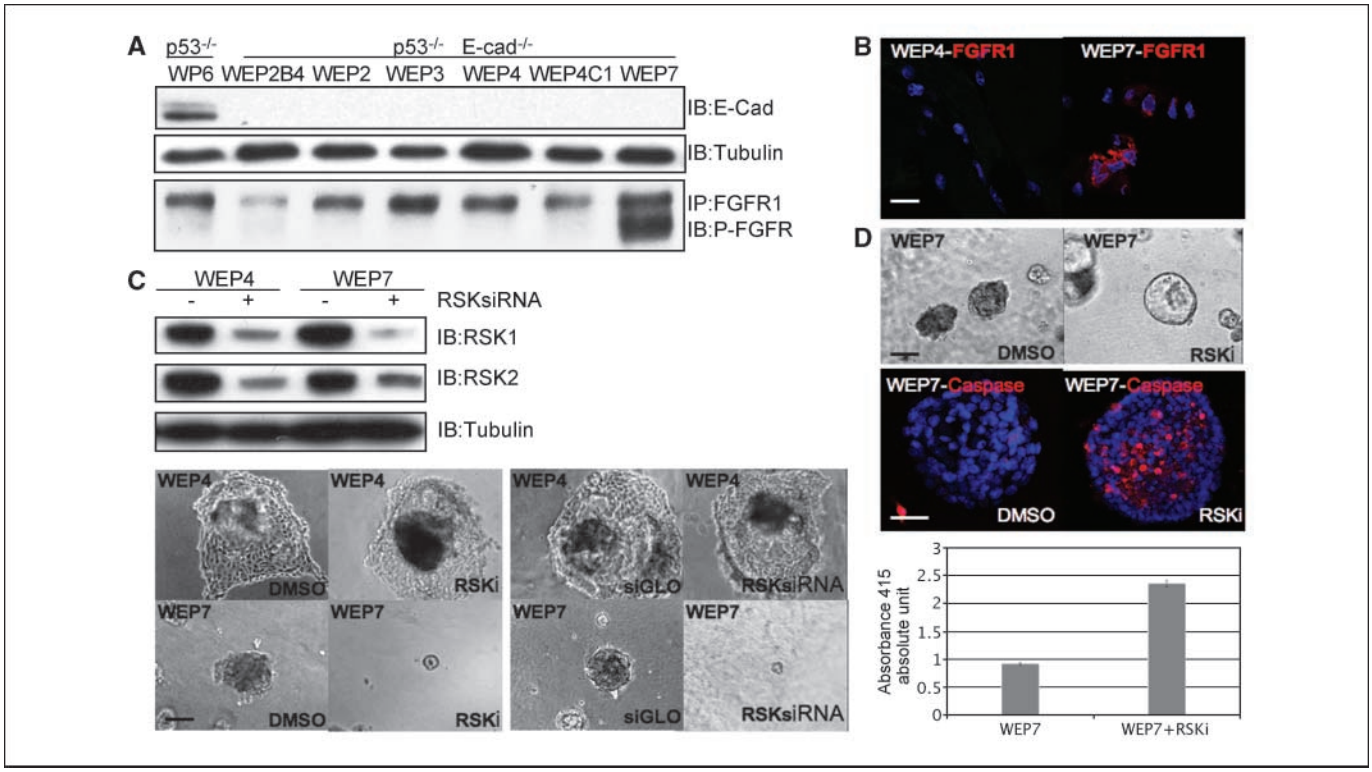

Figure 6. A murine lobular carcinoma cell line expressing FGFR1 is sensitive to RSK inhibition. *A,* Western blot of extracts of cell lines derived from seven tumors that arose in mice deficient for p53 or p53 and E-cadherin using antibodies to E-cadherin, tubulin, or phospho-FGFR ($Tyr^{653/654}$). *B,* immunofluorescence of tumor sections from WEP7 and WEP4 probed with anti-FGFR1 antibody (*red*) and DAPI (*blue*) to stain nuclei. *Bar,* 20 μm. *C, top,* Western blot of WEP4 and WEP7 tumor cell lines transfected with specific RSK siRNA using antibodies to RSK1 and RSK2; *bottom,* phase-contrast images of WEP7 and WEP4 cells grown on Matrigel with or without RSK inhibitor or RSK-specific siRNAs. *D, top,* images of WEP7 cells grown on Matrigel for 6 d and incubated with RSK inhibitor for an additional 6 d. Cleaved caspase-3 antibodies (*red*) and DAPI staining for nuclei (*blue*) are shown. *Bottom,* anoikis in WEP7 cells with and without RSK inhibitor. Apoptosis was measured using the Cell Death ELISA kit. Results are plotted as arbitrary units of absorbance at 405 nm. *Columns,* mean of triplicate from a representative experiment; *bars,* SD.

growth and survival specifically depend on RSK activity and, furthermore, that FGFR1-amplified tumors may exhibit "addiction" to RSK. The oncogene addiction phenomenon of cancer cells has been implicated in the success of targeted cancer therapies due to a novel, acquired dependence on a pathway by transformed cells (12, 14). Thus, RSK inhibitors may show selective activity against cancer cells expressing increased FGFR1 activity compared with normal cells.

Although these studies have highlighted the significance of RSK in FGFR1-expressing cells, many questions remain. Evidence exists for the role of cooperation of multiple RTKs in carcinomas. For example, it has been shown that in a subclass of breast cancers linked to aberrant expression of FGFR4 and ErbB2, simultaneous targeting of both receptors, but not either alone, may be an attractive therapeutic strategy (33). This raises the possibility that RSK, a common downstream component of many RTKs (20, 34), may represent a critical downstream target of multiple RTKs. It is likely that ongoing analysis of genetic lesions in tumors will reveal more information on the cooperative spectrum of tyrosine kinase receptors in cancers and potential benefits of targeting common downstream pathways. With regard to RSK inhibition, further *in vivo* preclinical models will be required to evaluate its potential significance in treating ILC and other types of human cancer linked to FGFR1 expression.

Disclosure of Potential Conflicts of Interest

No potential conflicts of interest were disclosed.

Acknowledgments

Received 9/5/2008; revised 10/28/2008; accepted 12/8/2008; published OnlineFirst 3/3/09.

Grant support: NIH grant CA089393 and Lee Jeans Translational Breast Cancer Research Program (J.S. Brugge) and Damon Runyon Cancer Innovation Award (N.S. Gray).

The costs of publication of this article were defrayed in part by the payment of page charges. This article must therefore be hereby marked *advertisement* in accordance with 18 U.S.C. Section 1734 solely to indicate this fact.

We thank Dr. Dhananjay Pendharkar and the chemists from SAI Advantium for help with chemical synthesis; Drs. John Blenis, Max Wicha, Fariba Behbod, Michael Overholtzer, and Ghassan Mouneimne for critical review and helpful discussions of the manuscript; ARIAD Pharmaceuticals, Inc. for their generous supply of dimerizer AP20187; and the Nikon Imaging Center at Harvard Medical School for imaging support.

References

1. Arpino G, Bardou VJ, Clark GM, Elledge RM. Infiltrating lobular carcinoma of the breast: tumor characteristics and clinical outcome. Breast Cancer Res 2004;6:R149–56.
2. Althuis MD, Dozier JM, Anderson WF, Devesa SS, Brinton LA. Global trends in breast cancer incidence and mortality 1973-1997. Int J Epidemiol 2005;34:405–12.
3. Smith DB, Howell A, Wagstaff J. Infiltrating lobular carcinoma of the breast: response to endocrine therapy and survival. Eur J Cancer Clin Oncol 1987;23:979–82.
4. Mathieu MC, Rouzier R, Llombart-Cussac A, et al. The poor responsiveness of infiltrating lobular breast carcinomas to neoadjuvant chemotherapy can be explained by their biological profile. Eur J Cancer 2004; 40:342–51.
5. Jirstrom K, Ryden L, Anagnostaki L, et al. Pathology parameters and adjuvant tamoxifen response in a randomised premenopausal breast cancer trial. J Clin Pathol 2005;58:1135–42.
6. Reis-Filho JS, Simpson PT, Turner NC, et al. FGFR1 emerges as a potential therapeutic target for lobular breast carcinomas. Clin Cancer Res 2006;12:6652–62.
7. Welm BE, Freeman KW, Chen M, Contreras A, Spencer DM, Rosen JM. Inducible dimerization of FGFR1: development of a mouse model to analyze progressive transformation of the mammary gland. J Cell Biol 2002; 157:703–14.
8. Xian W, Schwertfeger KL, Vargo-Gogola T, Rosen JM. Pleiotropic effects of FGFR1 on cell proliferation, survival, and migration in a 3D mammary epithelial cell model. J Cell Biol 2005;171:663–73.
9. Kang S, Dong S, Gu TL, et al. FGFR3 activates RSK2 to mediate hematopoietic transformation through tyrosine phosphorylation of RSK2 and activation of the MEK/ERK pathway. Cancer Cell 2007;12:201–14.
10. Shimamura A, Ballif BA, Richards SA, Blenis J. Rsk1 mediates a MEK-MAP kinase cell survival signal. Curr Biol 2000;10:127–35.
11. Smith JA, Poteet-Smith CE, Xu Y, Errington TM, Hecht SM, Lannigan DA. Identification of the first specific inhibitor of p90 ribosomal S6 kinase (RSK) reveals an unexpected role for RSK in cancer cell proliferation. Cancer Res 2005;65:1027–34.
12. Davies M, Hennessy B, Mills GB. Point mutations of protein kinases and individualised cancer therapy. Expert Opin Pharmacother 2006;7:2243–61.
13. Jonkers J, Berns A. Oncogene addiction: sometimes a temporary slavery. Cancer Cell 2004;6:535–8.
14. Sharma SV, Fischbach MA, Haber DA, Settleman J. "Oncogenic shock": explaining oncogene addiction through differential signal attenuation. Clin Cancer Res 2006;12:4392–5s.
15. Debnath J, Muthuswamy SK, Brugge JS. Morphogenesis and oncogenesis of MCF-10A mammary epithelial acini grown in three-dimensional basement membrane cultures. Methods 2003;30:256–68.
16. Nomura S, Yoshitomi H, Takano S, et al. FGF10/FGFR2 signal induces cell migration and invasion in pancreatic cancer. Br J Cancer 2008;99:305–13.
17. Muthuswamy SK, Li D, Lelievre S, Bissell MJ, Brugge JS. ErbB2, but not ErbB1, reinitiates proliferation and induces luminal repopulation in epithelial acini. Nat Cell Biol 2001;3:785–92.
18. Zhao H, Langerod A, Ji Y, et al. Different gene expression patterns in invasive lobular and ductal carcinomas of the breast. Mol Biol Cell 2004;15:2523–36.
19. Cohen MS, Zhang C, Shokat KM, Taunton J. Structural bioinformatics-based design of selective, irreversible kinase inhibitors. Science 2005;308:1318–21.
20. Anjum R, Blenis J. The RSK family of kinases: emerging roles in cellular signalling. Nat Rev Mol Cell Biol 2008;9:747–58.
21. McLeskey SW, Ding IY, Lippman ME, Kern FG. MDA-MB-134 breast carcinoma cells overexpress fibroblast growth factor (FGF) receptors and are growth-inhibited by FGF ligands. Cancer Res 1994;54:523–30.
22. Derksen PW, Liu X, Saridin F, et al. Somatic inactivation of E-cadherin and p53 in mice leads to metastatic lobular mammary carcinoma through induction of anoikis resistance and angiogenesis. Cancer Cell 2006;10:437–49.
23. Krause DS, Van Etten RA. Tyrosine kinases as targets for cancer therapy. N Engl J Med 2005;353:172–87.
24. Steeghs N, Nortier JW, Gelderblom H. Small molecule tyrosine kinase inhibitors in the treatment of solid tumors: an update of recent developments. Ann Surg Oncol 2007;14:942–53.
25. Ciardiello F, Tortora G. EGFR antagonists in cancer treatment. N Engl J Med 2008;358:1160–74.
26. Greenman C, Stephens P, Smith R, et al. Patterns of somatic mutation in human cancer genomes. Nature 2007;446:153–8.
27. Knowles MA. Novel therapeutic targets in bladder cancer: mutation and expression of FGF receptors. Future Oncol 2008;4:71–83.
28. Kwabi-Addo B, Ozen M, Ittmann M. The role of fibroblast growth factors and their receptors in prostate cancer. Endocr Relat Cancer 2004;11:709–24.
29. Grose R, Dickson C. Fibroblast growth factor signaling in tumorigenesis. Cytokine Growth Factor Rev 2005;16:179–86.
30. Bild AH, Yao G, Chang JT, et al. Oncogenic pathway signatures in human cancers as a guide to targeted therapies. Nature 2006;439:353–7.
31. Sapkota GP, Cummings L, Newell FS, et al. BI-D1870 is a specific inhibitor of the p90 RSK (ribosomal S6 kinase) isoforms *in vitro* and *in vivo*. Biochem J 2007; 401:29–38.
32. Cohen MS, Hadjivassiliou H, Taunton J. A clickable inhibitor reveals context-dependent autoactivation of p90 RSK. Nat Chem Biol 2007;3:156–60.
33. Koziczak M, Hynes NE. Cooperation between fibroblast growth factor receptor-4 and ErbB2 in regulation of cyclin D1 translation. J Biol Chem 2004;279: 50004–11.
34. Blenis J. Signal transduction via the MAP kinases: proceed at your own RSK. Proc Natl Acad Sci U S A 1993;90:5889–92.